Improvement of Photoinduced Birefringence Properties of Optically Active Methacrylic Polymers through Copolymerization of Monomers Bearing Azoaromatic Moieties

Luigi Angiolini,*,[†] Tiziana Benelli,[†] Loris Giorgini,[†] Elisabetta Salatelli,[†] Renato Bozio,[‡] Alessandro Daurù,[‡] and Danilo Pedron[‡]

Dipartimento di Chimica Industriale e dei Materiali and INSTM UdR-Bologna, Università di Bologna, Viale Risorgimento 4, 40136 Bologna, Italy, and Dipartimento di Scienze Chimiche and INSTM UdR-Padova, Università di Padova, Via Marzolo 1, 35131 Padova, Italy

Received October 14, 2005; Revised Manuscript Received November 25, 2005

ABSTRACT: Optically active photochromic copolymers of different composition, deriving from the conformationally rigid chiral monomer (*S*)-3-methacryloyloxy-1-(4′-nitro-4-azobenzene)pyrrolidine [(*S*)-MAP-N] and the isosteric and isopolar methacrylic ester of the flexible achiral chromophore 4′-[(2-hydroxyethyl)ethylamino]-4-nitrobenzene [DR1M], have been prepared and characterized in solution and in the solid state with the aim to investigate the effect on their thermal and chirooptical properties originated by the presence of isosteric and isopolar azoaromatic moieties in the side chain. The photoinduction of birefringence has been assessed on films of the investigated copolymers in order to evaluate their behavior as materials for optical data storage. The results are interpreted in terms of copolymer composition and different cooperative behavior and conformational stiffness of DR1M and (*S*)-MAP-N azoaromatic chromophoric counits.

Introduction

There is considerable interest in the synthesis and characterization of polymers containing azoaromatic moieties due to their unique optical properties.[1−9] They can be used in advanced micro- and nanotechnologies such as optical data storage,[10,11] nonlinear optical materials,[12,13] holographic memories,[14−16] chirooptical switches,[17,18] surface relief gratings,[19,20] etc.

Optically induced birefringence can be produced on these materials by linearly polarized (LP) photoexcitation of the azobenzene group, which undergoes trans−cis−trans isomerization[21,22] giving rise, after repeated photoexcitation and isomerization cycles, to a net excess of azobenzene moieties oriented with their transition dipole moments perpendicularly to the direction of the pump electric field. The anisotropic distribution of chromophores provides birefringence and linear dichroism of the film that can be erased by irradiation with depolarized or circularly polarized (CP) light, thus reproducing the original isotropy in the material.

On the other hand, the induction of chirality of helical in polymers or oligomers has attracted widespread interest because of possible applications in optical devices or data storage and also because of its relevance to chiral amplification as it may have occurred at the early stages of life.[23]

In this context, the presence of a chiral group of one prevailing configuration interposed between the polymeric backbone and the *trans*-azoaromatic chromophore provides the macromolecules with the further possibility to assume a conformational dissymmetry of one prevailing screw sense which can be revealed by the presence in the circular dichroism (CD) spectra of dichroic bands related to the electronic transitions of the chromophore. If electrostatic interactions are present between the *trans*-azoaromatic chromophores disposed according to a chiral geometry, it is also possible in the CD spectra to observe exciton splittings of the dichroic bands to an extent connected to the amount of the interactions present and hence to the overall amount of chiral conformations assumed by the macromolecules.[24−26]

In previous studies[27−29] we reported the synthesis and characterization of optically active photochromic homopolymeric derivatives bearing in the side chain a chiral pyrrolidinyl ring of one prevailing absolute configuration linked to a *trans*-azoaromatic system with permanent dipole moment. This functional combination allows the polymers to display both the properties typical of dissymmetric systems (optical activity, exciton splitting of chirooptical absorptions) and the features typical of photochromic materials (photorefractivity, photoresponsiveness, NLO properties). In addition, we have also observed[30,31] that it is possible to photomodulate the chirooptical properties of thin films of these chiral photochromic polymers by irradiation with CP light of one single L or R rotation sense. Although the mechanism responsible for the inversion of the CD signals is still presently under investigation,[32] this unexpected property seems to open new possibilities for the use of these materials as chirooptical switches, besides their usual applications in optics.

Recently, we have investigated the linear photoinduced optical properties of the homopolymer poly[(*S*)-3-methacryloyloxy-1-(4′-nitro-4-azobenzene)pyrrolidine] {poly[(*S*)-MAP-N]} (Scheme 1). As expected, poly[(*S*)-MAP-N] displays reversible linear dichroism and birefringence when irradiated with LP light followed by CP light.[30] As compared to poly(DR1M),[8,20] containing in the side-chain the flexible chromophore of Disperse Red 1 {4′-[(2-hydroxyethyl)ethylamino]-4-nitrobenzene} (Scheme 1), thoroughly investigated as material for optical data storage, poly[(*S*)-MAP-N] is characterized by enhanced photoinduced linear birefringence and long-term storage stability but displays lower stability to repeated cycles of irradiation.

With the aim to exploit the promising behavior and reduce the observed deficiencies of poly[(*S*)-MAP-N], we report in the

---

* Corresponding author: Tel and Fax +39 051 2093687; E-mail luigi.angiolini@unibo.it.

[†] Università di Bologna.

[‡] Università di Padova.

10.1021/ma052232u CCC: $33.50

Scheme 1

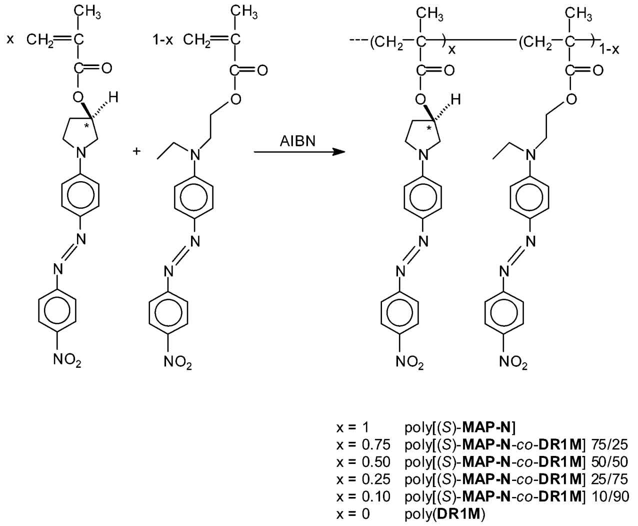

present paper an evaluation of the effects induced on the optical properties of this material by progressively distancing the photochromic chiral repeating units of (*S*)-MAP-N along the polymer backbone through copolymerization with known amounts of the isosteric and isopolar achiral comonomer DR1M. This has been achieved by radical copolymerization of these monomers in different molar amounts, so as to obtain the corresponding random copolymers poly[(*S*)-MAP-N-*co*-DR1M]s with a molar content of (*S*)-MAP-N of 10, 25, 50, and 75% (Scheme 1). The products have been fully characterized in solution and in the solid state as thin films, and the photomodulation of their photoinduced birefringence is discussed in terms of composition in view of their use for optical data storage.

Experimental Section

Materials. Disperse Red 1 (DR1) (Aldrich) was crystallized from ethanol/water 1:1 (v:v) before use. Methacryloyl chloride (Aldrich) was distilled (bp 95 °C) under dry nitrogen in the presence of traces of 2,6-di-*tert*-butyl-*p*-cresol as polymerization inhibitor before use. Triethylamine (Aldrich) was refluxed over dry $CaCl_2$ for 8 h and then distilled (bp 89 °C). 2,2′-Azobis(isobutyronitrile) (AIBN) (Aldrich) was crystallized from absolute ethanol before use.

Methylene dichloride, tetrahydrofuran (THF), *N*,*N*-dimethylformamide (DMF), and *N*,*N*-dimethylacetamide (DMA) were purified and dried according to reported procedures[33] and stored under nitrogen over molecular sieves (4 Å).

All other reagents and solvents (Aldrich) were used as received.

Monomers. (*S*)-3-Methacryloyloxy-1-(4′-nitro-4-azobenzene)-pyrrolidine [(*S*)-MAP-N] was prepared as previously reported[27] and crystallized from absolute ethanol; yield 47%, mp 166−168 °C. 4′-[[[2-(Methacryloyloxy)ethyl]ethyl]amino]-4-nitroazobenzene (DR1M) was synthesized by a procedure similar to that one described[8] using methylene dichloride as the solvent instead of tetrahydrofuran. The monomer was crystallized from absolute ethanol; yield 75%, mp 82−84 °C.

General Polymerization Procedure. Homo- and copolymerization reactions were carried out in glass vials using AIBN (2 wt % with respect to the monomers) as thermal initiator and dry THF as solvent (1 g of monomer in 15 mL of THF). Feeds of molar composition as reported in Table 1 were prepared and introduced into vials under a nitrogen atmosphere, submitted to several freeze−thaw cycles, and allowed to polymerize at 60 °C for 72 h. The polymerization process was stopped by pouring the reaction mixture into a large excess of methanol and the precipitate collected by filtration. The solid polymeric product was repeatedly redissolved in DMF and reprecipitated again with methanol. The last traces of unreacted monomers and oligomeric impurities were eliminated from the products by Soxhlet extraction with methanol. The material was finally dried to constant weight at 80 °C for 4 days under high vacuum. Relevant data for the synthesized products are reported in Table 1.

As an example, the spectroscopic data for poly[(*S*)-MAP-N-*co*-DR1M] 50/50 are here reported:

^1H NMR (in nitrobenzene-d_5 at 80 °C): 8.35−7.80 (m, 12H, arom ortho to nitro groups, arom 3-H and 2′-H), 7.10 (m, 2H, arom ortho to amino group of DR1M), 6.80 (m, 2H, arom ortho to amino group of (*S*)-MAP-N), 5.70−5.45 (m, 1H, pyrrolidine 3-CH), 4.20−3.50 (m, 8H, CH_3-CH_2-N and CH_2-CH_2-N of DR1M and pyrrolidine 2- and 5-CH_2), 2.60−1.10 ppm (m, 15H, pyrrolidine 4-CH_2, CH_3-CH_2-N of DR1M and backbone CH_3 and CH_2).

^{13}C NMR (in nitrobenzene-d_5 at 80 °C): 177.4−175.8 (CO), 157.3 (arom $C-NO_2$), 151.4, 148.7, 144.7 (arom $C-N=N-C$ and $C-N-CH_2$), 126.8 (arom 3′-C), 125.0, 123.3 (arom 2′-C and 3-C), 112.5 (arom 2-C), 75.4 (CH−O), 62.0 (CH_2-CH_2-O of DR1M), 55.2 (main chain CH_2-C), 53.2 ($CH-CH_2-N$), 47.1 (CH_2-CH_2-O of DR1M), 46.7 (CH_2-CH_2-N of (*S*)-MAP-N), 46.0 (main chain CH_2-C), 44.1 (CH_3-CH_2-N), 31.4 ($CH-CH_2-CH_2$), 20.2 and 18.5 (main chain CH_3), 11.5 ppm (CH_3CH_2-N).

FT-IR: 3105 and 3092 (ν_{CH}, arom), 2974, 2928, and 2854 (ν_{CH}, aliph), 1729 ($\nu_{C=O}$, ester), 1603 and 1516 ($\nu_{C=C}$, arom), 1131 (ν_{C-O}), 858 and 822 cm^{-1} (δ_{CH}, 1,4-disubst arom ring).

Physicochemical Measurements. The NMR spectra of monomers and low molecular weight intermediates were recorded with a Varian Gemini 300 spectrometer at room temperature on 5−10% solutions in $CDCl_3$. Polymeric derivatives were run at 80 °C in *p*-nitrobenzene-d_5 or at 90 °C in DMSO-d_6 solution in order to achieve a better signal resolution. Tetramethylsilane (TMS) was used as internal reference. ^1H NMR spectra were performed at 300 MHz, by using the following experimental conditions: 24 000 data points, 4.5 kHz spectral width, 2.6 s acquisition time, 16 transients. ^{13}C NMR spectra were recorded at 75.5 MHz, under full proton decoupling, by using the following experimental conditions: 24 000 data points, 20 kHz spectral width, 0.6 s acquisition time, 64000 transients.

FT-IR spectra were carried out on a Perkin-Elmer 1750 spectrophotometer, equipped with an Epson Endeavour II data station, on samples prepared as KBr pellets.

Number-average molecular weights of the polymers ($\bar{M}_n$) and polydispersity ($\bar{M}_w/\bar{M}_n$) were determined by size exclusion chromatography (SEC) in DMA solution eluted with THF using a HPLC Lab Flow 2000 apparatus, equipped with an injector Rheodyne 7725i, a Phenomenex Phenogel 5μ MXL column, and a UV−vis detector Linear Instruments model UVIS-200, working at 254 nm. Calibration curves were obtained by using several monodisperse polystyrene standards.

UV−vis absorption spectra of the samples were recorded at 25 °C on a Perkin-Elmer Lambda 19 spectrophotometer in the 250−650 nm spectral region in DMA solutions by using cell path lengths of 0.1 cm. Azobenzene chromophore concentrations of about 3×10^{-4} mol L^{-1} were used.

CD spectra of the samples were recorded at 25 °C on a Jasco 810A dichrograph, using the same spectral regions, cell path lengths, and concentrations as for UV measurements. $\Delta\epsilon$ values, expressed as L mol^{-1} cm^{-1}, were calculated by the following equation: $\Delta\epsilon = [\Theta]/3300$, where the molar ellipticity $[\Theta]$ in deg cm^2 $dmol^{-1}$ refers to one azobenzene chromophore.

Melting points (uncorrected) were determined in glass capillaries on a Büchi 510 apparatus at a heating rate of 1 °C/min.

The glass transition temperatures of polymers (T_g) were determined by differential scanning calorimetry (DSC) on a TA Instruments DSC 2920 modulated apparatus adopting a temperature program consisting of three heating and two cooling ramps starting from room temperature (heating/cooling rate 10 °C/min under a nitrogen atmosphere). Each sample (5−9 mg) was heated to below 250 °C in order to avoid thermal decomposition.

The initial thermal decomposition temperature (T_d) was determined on the polymeric samples with a Perkin-Elmer TGA-7 thermogravimetric analyzer by heating the samples in air at a rate of 20 °C/min.

Table 1. Characterization Data of Polymeric Derivatives

feed (mol %)			polymers				
(*S*)-MAP-N	DR1M	yield[a] (%)	(*S*)-MAP-N content[b] (mol %)	$\bar{M}_n$[c]	$\bar{M}_w/\bar{M}_n$[c]	T_d[d] (°C)	T_g[e] (°C)
100	0	74	100	21 200[f]	1.3[f]	315	208[f]
75	25	65	70	27 700	1.2	278	165
50	50	84	52	33 000	1.3	293	164
25	75	82	24	35 700	1.4	286	134
10	90	78	11	36 100	1.5	278	120
0	100	81	0	40 400[g]	1.5	295	121[g]

[a] Calculated as (g of polymer/g of monomer) × 100. [b] Determined by ^{1}H NMR. [c] Determined by SEC in THF solution at 25 °C. [d] Initial decomposition temperature determined by TGA in air at 20 °C/min heating rate. [e] Glass transition temperature determined by DSC under nitrogen at 10 °C/min heating rate. [f] Reference 27: $\bar{M}_n = 18\,300$; $\bar{M}_w/\bar{M}_n = 1.6$; $T_g = 208$ °C. [g] Reference 42: $\bar{M}_n = 4000$; $T_g = 129$ °C.

Amorphous thin films were prepared by spin-coating of a solution of the polymer in 1-methyl-2-pyrrolidinone/tetrahydrofuran (NMP/THF) onto clean glass slides. The films were then dried by heating above 80 °C under vacuum for 12 h. The film thickness, measured by a Tencor P-10 profilometer, was in the range 150−350 nm.

The native films resulted to be optically isotropic by inspection with a Zeiss Axioscope2 polarizing microscope through crossed polarizers fitted with a Linkam THMS 600 hot stage.

Absorption spectra of the films were carried out under the same instrumental conditions as the related solutions. The photoinduced linear birefringence was measured in situ using a pump and probe setup by monitoring the transmittance of the samples interposed between two crossed polarizers. The pump radiation at 488 nm was produced by a small frame Ar$^+$ laser, Spectra Physics model 165, whereas the source for the probe light was a Melles-Griot 10 mW He−Ne laser at 632.8 nm. The degree of linear polarization of the writing pump radiation was enhanced by using a Glan−Taylor prism polarizer, whereas a multiple order $\lambda/4$ quartz waveplate for 488 nm was employed to circularize the pump radiation for the erasing steps.

Results and Discussion

Synthesis and Characterization. Monomer (*S*)-MAP-N, having optical purity higher than 90%,[27] was submitted to copolymerization with DR1M under radical conditions in dry THF solution at 60 °C for 72 h. To complete the series, DR1M was also homopolymerized under the same conditions. All products were obtained in high yields, after purification, with high average molecular weight and comparable polydispersity values, as determined by SEC analysis.

The number-average molecular weight progressively decreases (Table 1) on passing from poly(DR1M) to poly[(*S*)-MAP-N]. This finding may be attributed, at least partially, to reduced solubility in THF of the derivatives containing higher relative amounts of (*S*)-MAP-N counits, which tend to precipitate from the solution during the polymerization process. Whereas the purified copolymers with a (*S*)-MAP-N content of 70% or lower were in fact sufficiently soluble in THF or hot CHCl$_3$, the homopolymer poly[(*S*)-MAP-N] was soluble in appreciable concentration only in strongly polar solvents such as hot nitrobenzene, DMF, DMA, or DMSO. This behavior is probably caused by the presence in the material of aggregates of the highly polar and rigid moieties of (*S*)-MAP-N.

The occurred polymerizations were confirmed by IR spectroscopy, by observing the disappearance in the spectra of the absorption bands at 1635−1636 cm^{-1}, related to the methacrylic double bonds, and the contemporary appearance of bands at 1729−1730 cm^{-1}, related to the carbonyl stretching vibration of the α,β saturated methacrylic ester group, shifted to higher frequency by ca. 10 cm^{-1} with respect to the monomeric precursor. Accordingly, in the ^{1}H NMR spectra of polymeric derivatives, shown in Figure 1, the resonances of the vinylidenic protons of the monomer were absent.

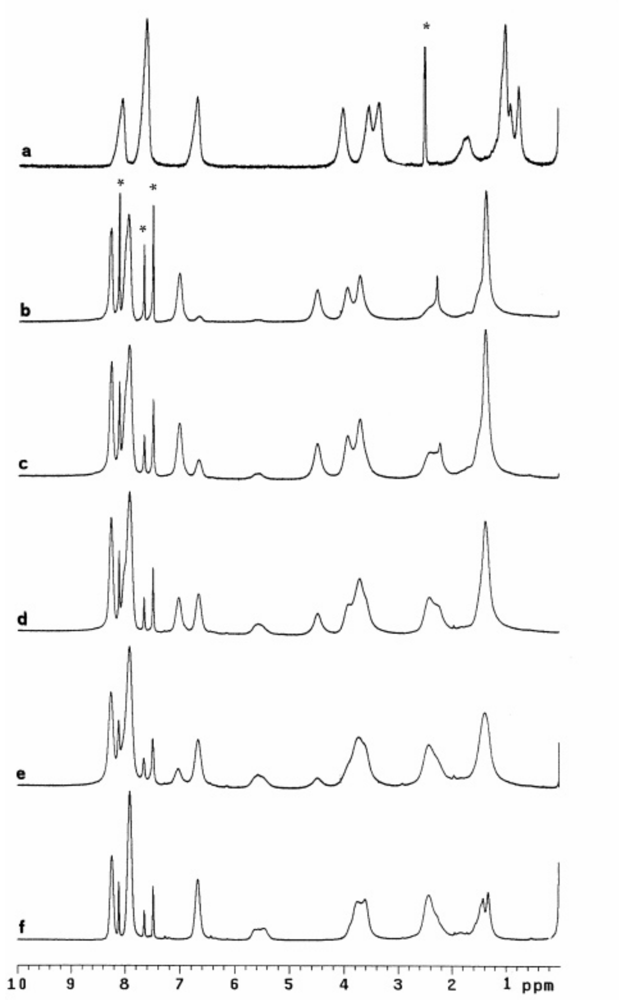

Figure 1. ^{1}H NMR spectra of poly(DR1M) (a) in DMSO-d_6 at 90 °C, poly[(*S*)-MAP-N-*co*-DR1M] 10/90 (b), poly[(*S*)-MAP-N-*co*-DR1M] 25/75 (c), poly[(*S*)-MAP-N-*co*-DR1M] 50/50 (d), poly[(*S*)-MAP-N-*co*-DR1M] 75/25 (e), and poly[(*S*)-MAP-N] (f) in nitrobenzene-d_5 at 80 °C. Starred signals refer to solvent resonances.

The molar composition of copolymers was also determined from ^{1}H NMR spectra (Figure 1) by comparing the integrated peak areas in both the aromatic and aliphatic regions of (*S*)-MAP-N and DR1M resonances. The averaged results are listed in Table 1.

The molar content of (*S*)-MAP-N in the copolymers roughly reflects the feed composition, indicating similar reactivities of the two methacrylate monomers. Indeed, as expected for methacrylates having similar structures, an approximate evaluation of the reactivity ratios performed by using the modified Kelen−Tüdos method[34,35] gives $r_{(S)-\mathrm{MAP-N}} = 0.51$ and $r_{\mathrm{DR1M}} = 0.71$, with a $r_{(S)-\mathrm{MAP-N}}r_{\mathrm{DR1M}}$ product of 0.36, indicative of a

Table 2. Mean Sequence Length ($\bar{l}$) and Molar Fraction $X_{(n)}$ (%) of (*S*)-MAP-N and DR1M Counits Having Sequence Length of *n* Units in Poly[(*S*)-MAP-N-*co*-DR1M]s

			$X_{(S)-\mathrm{MAP-N}(n)}$					$X_{\mathrm{DR1M}(n)}$				
sample	$\bar{l}_{(S)-\mathrm{MAP-N}}$	$\bar{l}_{\mathrm{DR1M}}$	$n = 1$	2	3	4	>4	$n = 1$	2	3	4	>4
copol 75/25[a]	3.03	1.18	10.8	14.5	14.6	13.1	46.8	72.1	21.7	4.9	1.0	0.2
copol 50/50[b]	1.41	1.87	50.0	29.3	12.8	5.0	2.8	28.5	26.6	18.6	11.5	14.8
copol 25/75[c]	1.18	2.97	71.4	22.1	5.1	1.0	0.2	11.3	15.0	14.9	13.2	45.5
copol 10/90[d]	1.05	8.44	90.9	8.4	0.6	0.0	0.0	1.4	2.5	3.3	3.8	89.0

[a] Poly[(*S*)-MAP-N-*co*-DR1M] at 70% molar content of (*S*)-MAP-N counits. [b] Poly[(*S*)-MAP-N-*co*-DR1M] at 52% molar content of (*S*)-MAP-N counits. [c] Poly[(*S*)-MAP-N-*co*-DR1M] at 24% molar content of (*S*)-MAP-N counits. [d] Poly[(*S*)-MAP-N-*co*-DR1M] at 11% molar content of (*S*)-MAP-N counits.

certain tendency to an alternating distribution of the counits along the polymer chain. As a consequence, the mean sequence lengths of the counits ($\bar{l}$) in the copolymers result short, as shown in Table 2, where the mean sequence lengths of the counits and the molar fractions of sequences of length *n* have been calculated utilizing the well-known methods reported in the literature.[36,37]

The microtacticity of synthesized copolymers, evaluated by integration of the ^{13}C NMR signals related to the methacrylic methyl group at about 20 and 18 ppm, belonging to *meso*−*racemo* (*mr*) and *racemo*−*racemo* (*rr*) triads,[38] respectively, indicates a content of syndiotactic (*rr*) triads around 50−55%, with a probability of formation of *meso* and *racemo* dyads of 0.26−0.28 and 0.72−0.74, respectively, in agreement with literature reports concerning the radical polymerization of MMA.[39] It is also confirmed that the addition of monomer (*S*)-MAP-N or DR1M to the growing chain is unaffected by the nature of the last repeating unit and follows Bernoullian statistics, as indicated by the close similarity of $P_{m/r}$ with $P_{m/m}$ and by the sum of $P_{m/r}$ with $P_{r/m}$ that gives 1.00, where $P_{m/r}$, $P_{r/m}$, $P_{m/m}$, and $P_{r/r}$ are the calculated probabilities that a given dyad follows a dyad having the same or the opposite relative configuration.

A lower stereoregularity degree (0.4 probability of forming *meso* dyads, very close to a random configuration distribution in the main chain) was previously reported[40] for poly(DR1M); however, the different synthetic procedure adopted and the lower value of average molecular weight (5000 g/mol) obtained may have affected the results.

Thermal Analysis. The thermal stability of all polymeric derivatives, as determined by thermogravimetric analysis (TGA), resulted very high, with decomposition temperature values (T_d) close to 300 °C (Table 1), much higher than that one reported for poly(MMA) (260 °C),[41] indicative of a remarkable presence of strong dipolar interactions in the solid state between the chromophores located in the macromolecular side chains and characterized by a high charge delocalization due to the presence of a donor−acceptor conjugated system. The T_d value for poly(DR1M), deeply investigated as polymeric material for optoelectronic applications, and here reported for the first time, is in the same range. Observation of polymeric derivatives with a polarizing microscope did not reveal any liquid crystalline behavior.

Only second-order transitions originated by glass transitions, with no melting peaks, are observed in the DSC thermograms of the investigated polymers (Table 1), thus suggesting that the macromolecules are substantially amorphous in the solid state. The T_g values appear quite high, except for the sample poorest in (*S*)-MAP-N moieties, laying in the range 140−200 °C, that can be of great interest for applications in optoelectronics (more stable photoinduced birefringence, etc.). In particular, they are considerably higher than those measured for poly(DR1M) here (121 °C) and reported by Natansohn[42] for the same polymer with different average molecular weight and polydispersity (129 °C).

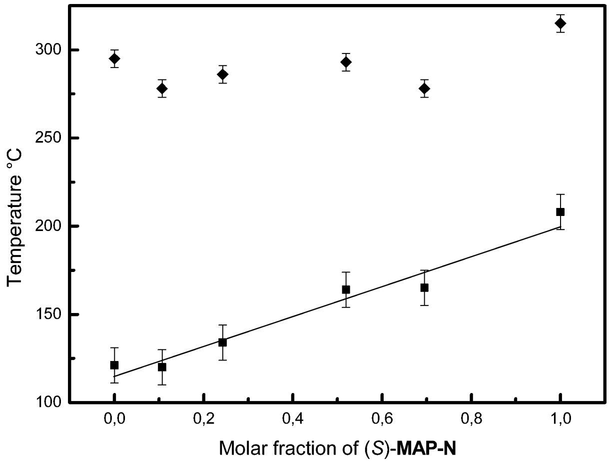

Figure 2. Dependence of the glass transition temperature (■) and of the initial decomposition temperature (◆) of polymeric derivatives in function of the (*S*)-MAP-N content.

This behavior is indicative of much reduced mobility of the macromolecular chains containing (*S*)-MAP-N, originated by the presence both of the conformational rigid pyrrolidine ring interposed between the backbone and the azoaromatic chromophore and of extended interchromophore dipolar interactions in the solid state. Indeed, the T_g values of homo- and copolymers increase considerably and almost linearly with increasing the (*S*)-MAP-N content (Figure 2), high values of T_g being required in order to achieve enhanced temporal stability at room temperature of the photo- or electrically oriented dipoles in the bulk.

Absorption Spectra. The UV−vis spectra of the polymers in *N*,*N*-dimethylacetamide (DMA) solution exhibit in the 250−650 nm spectral region (Table 3) two absorption bands, centered at about 470−480 and 290 nm, and related, the former, to combined n−π*, π−π*, and internal charge-transfer electronic transitions of the conjugated azoaromatic chromophore and the latter to the π−π* electronic transition of the aromatic ring.[43]

The spectroscopic properties in solution of copolymers poly[(*S*)-MAP-N-*co*-DR1M]s are quite similar to those exhibited by both the respective homopolymers poly[(*S*)-MAP-N] and poly(DR1M). As regards the first absorption band, an hypochromic effect can be generally observed when the spectra of the low molecular weight model compound (*S*)-3-pivaloyloxy-1-(4′nitro-4-azobenzene) pyrrolidine [(*S*)-PAP-N][27] and of monomer DR1M, where the lack of structural restraints originates a random distribution in dilute solution of the chromophores, are compared with those of the related homopolymers and the copolymers (Table 3). Such a behavior, frequently noticed in polymeric derivatives bearing side-chain aromatic chromophores,[25−27,44,45] is attributed to the presence of electrostatic dipolar interactions between adjacent chromophores.[46−48] Analo-

Table 3. UV Spectra in DMA Solution of Polymers, (*S*)-PAP-N and DR1M

sample	first absorption band		second absorption band	
	λ_{max}[a]	$\epsilon_{max} \times 10^{-3}$ [b]	λ_{max}[a]	$\epsilon_{max} \times 10^{-3}$ [b]
(*S*)-PAP-N[c]	491	33.8	287	11.1
poly[(*S*)-MAP-N][c]	472	28.0	287	11.1
poly[(*S*)-MAP-N-*co*-DR1M]75/25	478	29.6	286	11.4
poly[(*S*)-MAP-N-*co*-DR1M]50/50	476	29.8	287	11.2
poly[(*S*)-MAP-N-*co*-DR1M]25/75	478	30.3	286	11.4
poly[(*S*)-MAP-N-*co*-DR1M]10/90	478	32.5	285	12.3
poly(DR1M)	479	29.3	285	11.0
DR1M	490	32.6	286	11.2

[a] Wavelength of maximum absorbance, expressed in nm. [b] Expressed in L mol^{-1} cm^{-1} and calculated for one single chromophore. [c] Reference 27.

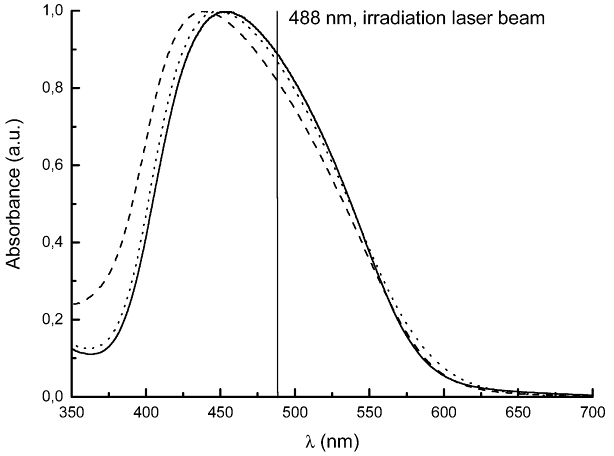

Figure 3. UV−vis absorption spectra of a 130 nm thick film of poly[(*S*)-MAP-N] (- - -), 240 nm thick film of poly[(*S*)-MAP-N-*co*-DR1M] 50/50 (• • •), and 320 nm thick film of poly(DR1M) (—) on fused silica.

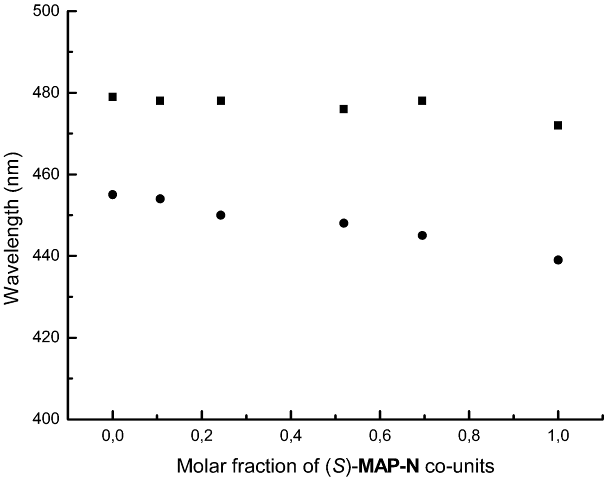

Figure 4. Dependence of the maximum absorption wavelength of the polymers in DMA solution (■) and as thin film (●) on the (*S*)-MAP-N content.

gously, the blue shift of the maximum absorption wavelength on passing from the low molecular weight compounds to the polymers, more evident when comparing (*S*)-PAP-N to poly[(*S*)-MAP-N], can be ascribed to the same reason, as previously reported.[27,49]

In first approximation, the behavior of the copolymeric systems in solution suggests that their electronic transitions are substantially unaffected by the presence in the side chain of different counits.

The electronic spectra of native thin films of poly[(*S*)-MAP-N], poly(DR1M), and the copolymer poly[(*S*)-MAP-N-*co*-DR1M] 50/50 normalized for thickness are shown in Figure 3. The amorphous polymers in the solid state exhibit strong absorptions in the visible and UV region centered at about 440−455 and 290 nm, respectively, assigned to the same electronic transitions observed in solution. Similarly to the solution, the visible absorption maximum wavelength moves to shorter wavelengths (blue shift) as the (*S*)-MAP-N content increases (Figure 4), but with a larger total shift (about 16 nm) with respect to the DMA solution (about 7 nm).

According to several reports,[50−52] this behavior is attributed to an increase of the intramolecular parallel arrangement of the neighboring adjacent electric dipoles (H-type aggregation) imposed by the structural constraints of the macromolecules[30] when the solvent is removed and the polymer chains collapse to form the film.

In solution, most of the azoaromatic dipoles are surrounded by the solvent (dielectric constant of DMA 37.8 at 20 °C[53]), this effect causing a shift of the absorption maximum to longer wavelengths and reducing at the same time the interactions between dipoles; thus, the blue shift originated by dipole−dipole interaction is lower in solution than in the film. This suggests that the observed blue shift should be a consequence of intramolecular interactions among chromophores and confirms that the aggregation between (*S*)-MAP-N counits is stronger than that one between DR1M counits, the interactions between (*S*)-MAP-N and DR1M moieties in the copolymers being of intermediate strength.

Chirooptical Properties. Recently[27] we have observed that the CD spectra of poly[(*S*)-MAP-N], both in DMA solution and as thin film, are characterized in the visible region by two intense dichroic signals of opposite sign and similar intensity with a crossover point roughly corresponding to the first absorption maximum. These signals, which are related to the electronic transitions shown in the absorption spectra by the azobenzene chromophores, are absent in the spectra in solution of the corresponding low molecular weight model compound, (*S*)-PAP-N, representative of the repeating unit of the polymer. This behavior is typical of exciton splitting determined by cooperative dipole−dipole interactions between neighboring side chain azobenzene chromophores arranged in a mutual chiral geometry of one prevailing handedness.[24−28] The presence of a rigid chiral moiety of one prevailing absolute configuration, interposed between the main chain of the polymer and the azoaromatic chromophore, favors the adoption of a chiral conformation of one prevailing helical handedness, at least for chain segments of the macromolecules in solution and is persistent also in the solid state.

The intensities of dichroic absorptions in DMA solution decrease upon decreasing the content of optically active (*S*)-MAP-N counits (Table 4 and Figure 5), thus confirming that the presence of achiral isosteric DR1M counits progressively reduces the extent of the interactions between dipoles ordered according to a chiral arrangement, with respect to the related homopolymer deriving from (*S*)-MAP-N.

Table 4. CD Spectra in DMA Solution of Polymeric Derivatives and (*S*)-PAP-N

	first absorption band					second absorption band	
sample	$\lambda_1{}^a$	$\Delta\epsilon_1{}^b$	$\lambda_0{}^c$	$\lambda_2{}^a$	$\Delta\epsilon_2{}^b$	$\lambda_3{}^a$	$\Delta\epsilon_3{}^b$
poly[(*S*)-MAP-N][d]	518	+9.00	469	433	−6.28	285	−0.37
poly[(*S*)-MAP-N-*co*-DR1M]75/25	518	+5.37	474	439	−3.31	n. d.[e]	n. d.[e]
poly[(*S*)-MAP-N-*co*-DR1M]50/50	519	+3.56	472	436	−1.69	n. d.[e]	n. d.[e]
poly[(*S*)-MAP-N-*co*-DR1M]25/75	513	+1.27	468	448	−0.30	n. d.[e]	n. d.[e]
poly[(*S*)-MAP-N-*co*-DR1M]10/90	487	+0.76				n. d.[e]	n. d.[e]
(*S*)-PAP-N[d]	495	−0.67				284	+0.28

[a] Wavelength (in nm) of maximum dichroic absorption. [b] $\Delta\epsilon$ expressed in L mol^{-1} cm^{-1} and calculated for one repeating unit in the polymer. [c] Wavelength (in nm) of the crossover of dichroic bands. [d] Reference 27. [e] Not determined due to low intensity of the signals.

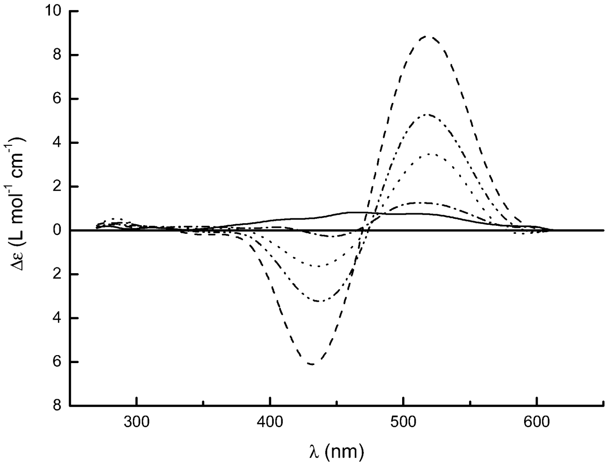

Figure 5. CD spectra in DMA of poly[(*S*)-MAP-N-*co*-DR1M]s at 11% (—), 24% (- • -), 52% (• • •) and 70% (- •• -) molar content of (*S*)-MAP-N counits and of poly[(*S*)-MAP-N] (- - -).

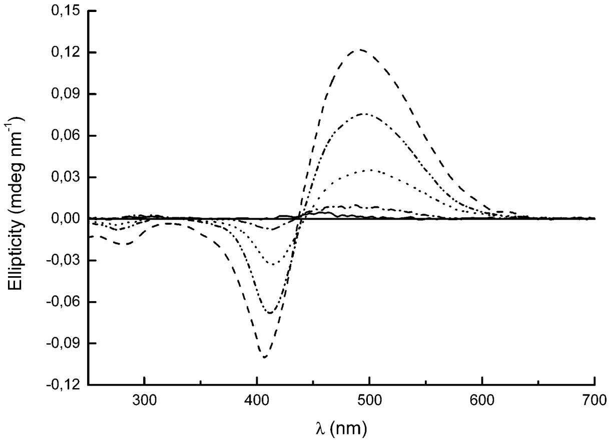

Figure 6. CD spectra of thin films of poly[(*S*)-MAP-N-*co*-DR1M]s at 11% (—), 24% (- • -), 52% (• • •) and 70% (- •• -) molar content of (*S*)-MAP-N counits and of poly[(*S*)-MAP-N] (- - -).

In other words, although relevant dipolar interactions between the azoaromatic moieties of (*S*)-MAP-N and DR1M are present, as observed by UV spectroscopy, the chiral counits of (*S*)-MAP-N appear substantially unable to maintain the conformational dissymmetry of the optically active homopolymer, when achiral counits of DR1M are also present along the main chain.

It can be noted that an exciton splitting is well visible at a molar content of chiral azoaromatic chromophore as low as 24% and that the copolymer of the lowest composition (11%) shows a shape tendentially similar to the model (*S*)-PAP-N, that exhibits in dilute solution a completely disordered distribution of chromophores with consequent absence of any couplet and optically active conformational order (Table 4 and Figure 5).

This behavior was previously also observed in analogous optically active copolymers of (*S*)-MAP-N with methyl methacrylate,[54] differently from the well-known case of polyisocyanates, where the introduction of even small amounts of chiral units in the side chain forces the achiral ones to adopt a helical conformation of the same sense as that one of the chiral moieties (the so-called sergeant and soldier copolymers).[55] The investigated copolymers have comparable stereoregularity of the main chain, as reported in Table 3; that however does not give any contribution to the overall optical activity of the macromolecules, the optical activity displayed by copolymeric derivatives being only ascribed to the presence of conformational dissymmetry between adjacent (*S*)-3-hydroxypyrrolidine azoaromatic repeating units, at least for chain sections.

Considering the mean sequence lengths of the chiral counits and their molar fractions, reported in Table 2, it appears that even few adjacent chiral units or a low fraction of sequences of sufficiently high length are able to produce a remarkable optical activity in the macromolecules. In fact, the copolymer poly[(*S*)-MAP-N-*co*-DR1M] at 11% molar content of (*S*)-MAP-N already shows an optical activity appreciably larger than the model compound (*S*)-PAP-N, although it is constituted by 90.9% of isolated units and only the 0.6% of sequences of three repeating units.

The CD spectra of amorphous thin films of poly[(*S*)-MAP-N] (130 nm thick, dashed line) and copolymers poly[(*S*)-MAP-N-*co*-DR1M]s, as represented in Figure 6 and expressed in terms of ellipticity normalized for thickness, are quite similar to those shown by the same polymers in solution (Figure 5 and Table 4).

In accordance with the absorption spectra, a blue shift of the CD bands is observed on passing from the solution to the solid state. The close similarity between the CD spectra of the native polymer films and those of the polymers in solution suggests that the macromolecules maintain chiral conformations of one prevailing helical handedness also in the solid amorphous state, at least for chain segments.

Studies concerning the photomodulation of their chirooptical properties in the solid state by using one handed-CP irradiation light are currently in progress.

Optical Storage Experiments. It is well-known that a good matching of the absorption wavelength with the wavelength of the pumping laser has a positive effect on storage efficiency.[1,20] Being the absorption spectra of the investigated polymers quite similar, a laser light operating at 488 nm, in resonance with their intense electronic transition in the visible (Figure 3), has been used in the irradiation experiments in order to gain the same pumping efficiency. To assess the presence of photoinduced linear dichroism and birefringence, films of the polymers have been irradiated with linearly polarized (LP) radiation (writing step) at 488 nm ($I \approx 100$ mW cm^{-2}). After irradiation, the samples show high photoinduced linear birefringence due to linear ordering of the azoaromatic moieties, as evidenced by using a probe radiation at 632.8 nm ($I \approx 1$ mW cm^{-2}), where the polymers have negligible absorption. The photoinduced

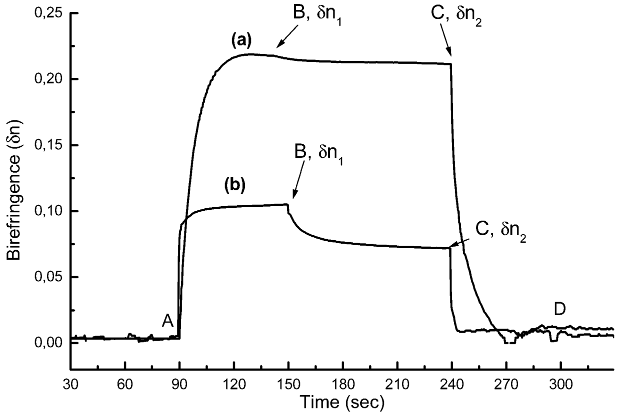

Figure 7. Complete writing-erasing cycle on a 130 nm thick film of poly[(*S*)-MAP-N] (a) and 320 nm thick film of poly(DR1M) (b) on fused silica. The LP radiation at 488 nm was switched on at point A and switched off at point B. The birefringence signal turns to zero by irradiating with CP light at point C; at point D the erasing CP light was turned off.

birefringence can be reversibly erased by using circularly polarized (CP) or depolarized pump radiation (erasing step).

In a recent preliminary investigation we have compared the photoinduced linear optical properties of poly[(*S*)-MAP-N] with poly(DR1M).[30] After irradiation with LP light, poly[(*S*)-MAP-N] shows a saturated photoinduced linear birefringence $|\delta n_1|$ of 0.218, which, after removal of the pump, relaxes to a stable value $|\delta n_2|$ of 0.211, as reported in Figure 7. The relaxation is of small extent, with $S = 0.97$ (where S is the relaxation coefficient expressed as the ratio $\delta n_2/\delta n_1$), and the induced anisotropy is stable for several months. These observed values are larger than those obtained, in the same experimental conditions, for poly(DR1M)[8,20] (Figure 7), which shows a saturated linear birefringence of 0.10 under illumination and 0.08 after removal of the pump, in very good agreement with the literature report[8] ($|\delta n_1|$ of 0.103 under illumination and $|\delta n_2|$ of 0.08 after pump removal). The relatively high birefringence relaxation of poly(DR1M) ($S = 0.80$) is due to some chromophoric moieties which do not remain oriented on a long-term basis, as exhaustively discussed by the authors.[20]

In comparison to poly(DR1M), the chiral homopolymer poly-[(*S*)-MAP-N] is characterized by enhanced photoinduced linear birefringence and long-term storage stability but displays slower writing/erasing response and low stability to repeated cycles of irradiation. As shown by profilometric measurements, when irradiated several times and for a long time with a single laser beam, the macromolecular chains migrate in concert with the photoalignment of the chromophores. This macroscopic mass transport produces a deformation of the film that prevents the possibility of its use for many writing−erasing steps, although it may be promising for fabrication of surface relief grating (SRG).[56]

The copolymers containing both (*S*)-MAP-N and DR1M counits display intermediate properties according to their composition, with respect to the related homopolymers, as clearly shown in Figure 8. The dependence of photoinduced birefringence on composition of homo- and copolymeric derivatives indicates the presence of two trends connected with the relative content of repeating units bearing the rigid pyrrolidinyl ring or the flexible DR1M moiety in the side chain. For example, the copolymer poly[(*S*)-MAP-N-*co*-DR1M] with 70% molar content of (*S*)-MAP-N shows photoinduced properties similar to poly[(*S*)-MAP-N]. As this copolymer has a mean sequence length of chiral counits of 3.03, with isolated units of DR1M (Table 2), this suggests that even few adjacent counits of (*S*)-MAP-N are able to produce a remarkable macroscopic cooperative photoinduced effect on the material. By contrast, all the copolymers with lower molar content of (*S*)-MAP-N counits show a behavior similar to that of poly(DR1M), as far as the birefringence values are concerned.

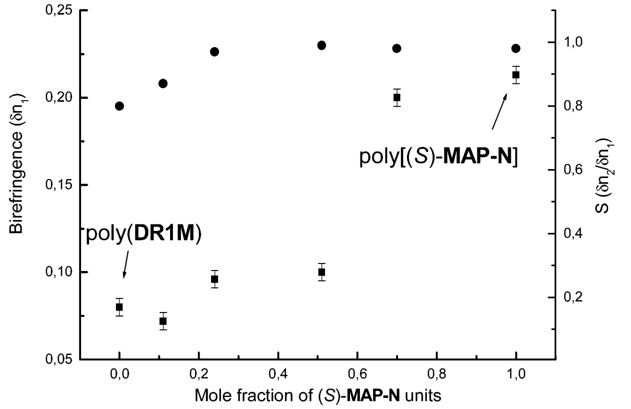

Figure 8. Stable photoinduced birefringence (δn_1) (■) and relaxation coefficient ($S = \delta n_2/\delta n_1$) (●) of the investigated polymers as a function of molar fraction content of (*S*)-MAP-N.

On the other side, the copolymer poly[(*S*)-MAP-N-*co*-DR1M] 10/90 displays a rapid increase of $|\delta n_1|$, with writing rate constants similar to poly(DR1M),[20] and then a slow growth to the saturation level of 0.08 (Figure 8). When the pumping light is turned off, a relaxation to the stable value of $|\delta n_2| = 0.07$ occurs, with a birefringence relaxation coefficient of 0.87, higher than that of poly(DR1M). Poly[(*S*)-MAP-N-*co*-DR1M] 25/75 gives a $|\delta n_1|$ of 0.10, which persists when the orientating LP light is switched off, with a ratio $|\delta n_2|/|\delta n_1|$ of about 1 (Figure 8). A closely similar behavior is observed for poly[(*S*)-MAP-N-*co*-DR1M] 50/50 (Figure 8). In other words, the chromophoric moieties remain oriented on a long-term basis, maintaining, in the time, the optical information written over the material. The induced anisotropy is observed to stay stable for several months and can be reversibly erased by using CP pump radiation at 488 nm at room temperature. Moreover, the copolymers with a molar content of (*S*)-MAP-N ranging from 52 to 11% are characterized by writing/erasing rate constants similar to those of poly(DR1M).

As mentioned above, no significant differences were observed between the copolymeric sample having 70% molar content of (*S*)-MAP-N with respect to poly[(*S*)-MAP-N] both under illumination and after pump removal. This behavior, not directly related to the value of T_g, which increases with the molar fraction of (*S*)-MAP-N counits (Table 1), suggests that the observed photoinduced linear birefringence may be due to similar cooperative motions as those well-known for side-chain liquid crystalline polymers, which are driven, in that case, by a thermodynamic tendency of chromophores to assume an ordered alignment. Copolymers poly[(*S*)-MAP-N-*co*-DR1M]s appear, however, completely amorphous both before and after the irradiation steps, as checked by polarizing microscopy, and the driving force for the observed cooperative effect may be due to the dissimilar electrostatic dipolar interactions between adjacent (*S*)-MAP-N and DR1M chromophores (as evidenced by the absorption spectra) or to steric factors (free volume necessary for the motion of azo groups), or to a combination of both.

For data storage applications, it is important to know how the photoinduced birefringence decays (relaxation coefficient *S*) and which level of photoinduced signal will be stable for a long time.

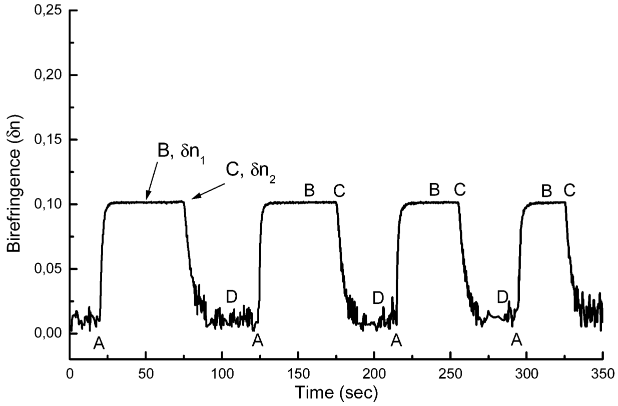

Figure 9. Multiple writing−erasing cycles on a 195 nm thick film of poly[(*S*)-MAP-N-*co*-DR1M] 50/50 on fused silica. A, B, C, D as in Figure 7.

In this context, it appears that the investigated copolymers are characterized by enhanced long-term stability of the photoinduced linear birefringence with respect to poly(DR1M), which can be attributed to the different chromophoric structure:[20] the azoaromatic moiety in poly(DR1M), in fact, is bonded to the backbone through a flexible spacer and may rapidly relax to its original isotropic state; by contrast, in (*S*)-MAP-N counits, one of the aromatic rings is conformationally hindered by the pyrrolidine ring so that its free rotation is probably reduced. Indeed, the reduced mobility of the macromolecular chains, originated by the presence of the conformationally rigid pyrrolidine ring interposed between the azoaromatic group and the methacrylic main chain, improves the T_g values as discussed above. As a consequence, the photoinduced birefringence in the copolymers containing the (*S*)-MAP-N moiety remains stable for a longer time than in polymers such as poly(DR1M). Actually, all copolymeric derivatives having a molar content of (*S*)-MAP-N counits above the 24% show a similar long-term stability, which persists for at least 6 months and is well reproducible.

The complete reversibility of the photoinduced linear birefringence of the investigated copolymers, which is related to fatigue resistance properties, as shown in Figure 9, seems to be promising for use in optical storage or more generally in the field of photoresponsive systems. Indeed, after several irradiations steps with LP and CP laser beams alternatively acting on the film, the values of maximum photoinduced birefringence and erased birefringence are quite similar. This indicates that no degradation photoreactions or relevant mass motions take place on irradiation by laser light of relatively high intensity (100 mW/cm^2). Thus, several cycles could be performed without any significant change in the photoinduced behavior.

Conclusions

Optically active photochromic copolymers deriving from the azoaromatic monomers (*S*)-MAP-N and DR1M have been prepared in a wide range of compositions and fully characterized. The presence in the macromolecules of the conformationally rigid (*S*)-MAP-N counits allows to achieve T_g values, higher than that of the homopolymer poly(DR1M), deeply investigated as polymeric material for optical storage, which can be of interest for applications in optoelectronics, even at a 24% molar content of (*S*)-MAP-N moieties.

The CD spectra of the investigated copolymers are characterized by intense dichroic signals related to the electronic transitions of the azobenzene chromophores. The presence in the spectra of exciton splittings is typical of cooperative interactions between the chromophores disposed in a mutual chiral geometry of one prevailing handedness. This indicates that the macromolecules assume chiral conformations of one prevailing helical sense, at least for chain sections. However, the (*S*)-MAP-N chiral units appear substantially unable to maintain the extent of conformational dissymmetry typical of the homopolymer poly[(*S*)-MAP-N], when the flexible achiral counits of DR1M are also present along the main chain.

While poly[(*S*)-MAP-N] is characterized by enhanced photoinduced linear birefringence and lower relaxation after pump removal with respect to poly(DR1M), but lower stability to repeated cycles of irradiation, the copolymers with a molar content of (*S*)-MAP-N moieties ranging from 11 to 52% display an improved birefringence relaxation coefficient, the chromophoric moieties remaining oriented for a long time, thus allowing the storage of the optical information written over the material. In addition, the copolymers exhibit stability to repeated cycles of irradiation at a molar content of (*S*)-MAP-N counits as low as 11%.

Acknowledgment. The financial support by MIUR (PRIN2004) and Consortium INSTM (FIRB2001 “RBNE01P4JF”) is gratefully acknowledged.

References and Notes

(1) *Proceedings of the Symposium on Azobenzene-Containing Materials, Boston, MA, 1998;* Natansohn, A., Ed.; *Macromol. Symp.* **1999**, *137*, 1−165.
(2) Natansohn, A.; Rochon, P.; Ho, M. S.; Barrett, C. *Macromolecules* **1995**, *28*, 4179.
(3) Wu, Y.; Zhang, Q.; Kanazawa, A.; Shiono, T.; Ikeda, T.; Nagase, Y. *Macromolecules* **1999**, *32*, 3951.
(4) Maertens, C.; Dubois, P.; Jerome, R.; Blanche, P. A.; Lemaire, P. C. *J. Polym. Sci., Part B: Polym. Phys.* **2000**, *38*, 205.
(5) Mendonca, C. R.; Dhanabalan, A.; Balogh, D. T.; Misoguti, L.; dos Santos, D. S., Jr.; Pereira-da-Silva, M. A.; Giacometti, J. A.; Zilio, S. C.; Oliveira, O. N., Jr. *Macromolecules* **1999**, *32*, 1493.
(6) Kim, J. H.; Kumar, S.; Lee, S. D. *Phys. Rev. E* **1998**, *57*, 5644.
(7) Ichimura, K. *Chem. Rev.* **2000**, *100*, 1847.
(8) Natansohn, A.; Rochon, P.; Gosselin, J.; Xie, S. *Macromolecules* **1992**, *25*, 2268.
(9) Han, M.; Morine, S.; Ichimura, K. *Macromolecules* **2000**, *33*, 6360.
(10) Gibbons, W. M.; Shannon, P. J.; Sun, S. T.; Swetlin, B. J. *Nature (London)* **1991**, *351*, 49.
(11) Holme, N. C. R.; Ramanujam, P. S.; Hvilsted, S. *Opt. Lett.* **1996**, *21*, 902.
(12) Katz, H.; Singer, K.; Sohn, J.; Dirk, C. *J. Am. Chem. Soc.* **1987**, *109*, 6561.
(13) Delaire, J. A.; Nakatani, K. *Chem. Rev.* **2000**, *100*, 1817.
(14) Todorov, T.; Nikolova, L.; Tomova, N. *Appl. Opt.* **1984**, *23*, 4588.
(15) Andruzzi, L.; Altomare, A.; Ciardelli, F.; Solaro, R.; Hvilsted, S.; Ramanujam, P. S. *Macromolecules* **1999**, *32*, 448.
(16) Eich, M.; Wendorff, J. H.; Reck, B.; Ringsdorf, H. *Macromol. Chem. Rapid Commun.* **1987**, *8*, 56.
(17) Iftime, G.; Labarthet, F. L.; Natansohn, A.; Rochon, P. *J. Am. Chem. Soc.* **2000**, *122*, 12646.
(18) Verbiest, T.; Kauranen, M.; Persoon, A. J. *Mater. Chem.* **1999**, *9*, 2005.
(19) Wu, Y.; Natansohn, A.; Rochon, P. *Macromolecules* **2004**, *37*, 6090−6095.
(20) Natansohn, A.; Rochon, P. *Chem. Rev.* **2002**, *102*, 4139−4175.
(21) Jones, C.; Day, S. *Nature (London)* **199**, *351*, 15.
(22) Sekkat, Z.; Wood, J.; Knoll, W. *J. Phys. Chem.* **1995**, *99*, 17226.
(23) Green, M. M.; Peterson, N. C.; Sato, T.; Teramoto, A.; Cook, R.; Lifson, S. *Nature (London)* **1995**, *268*, 1860.
(24) Carlini, C.; Angiolini, L.; Caretti, D. Photochromic Optically Active Polymers. In *Polymeric Materials Encyclopedia*; Salamone, J. C., Editor-in-Chief; CRC Press: Boca Raton, FL, 1996; Vol. 7, pp 5116−5123.
(25) Angiolini, L.; Caretti, D.; Giorgini, L.; Salatelli, E. *Macromol. Chem. Phys.* **2000**, *201*, 533.
(26) Angiolini, L.; Caretti, D.; Giorgini, L.; Salatelli, E.; Altomare, A.; Carlini, C.; Solaro, R. *Polymer* **1998**, *39*, 6621.
(27) Angiolini, L.; Caretti, D.; Giorgini, L.; Salatelli, E. *J. Polym. Sci., Part A: Polym. Chem.* **1999**, *37*, 3257.
(28) Angiolini, L.; Caretti, D.; Giorgini, L.; Salatelli, E. *Polymer* **2001**, *42*, 4005.

(29) Angiolini, L.; Giorgini, L.; Salatelli, E. *e-Polym.* **2003**, no. 037.
(30) Angiolini, L.; Bozio, R.; Giorgini, L.; Pedron, D.; Turco, G.; Daurù, A. *Chem.—Eur. J.* **2002**, *8*, 4241.
(31) Angiolini, L.; Benelli, T.; Bozio, R.; Daurù, A.; Giorgini, L.; Pedron, D. *Synth. Met.* **2003**, *139*, 743.
(32) Angiolini, L.; Benelli, T.; Giorgini, L.; Painelli, A.; Terenziani, F. *Chem.—Eur. J.* **2005**, *11*, 6053.
(33) Perrin, D. D.; Amarego, W. L. F.; Perrin, D. R. *Purification of Laboratory Chemicals*; Pergamon Press: Oxford, 1966.
(34) Kelen, T.; Tüdos, F. *J. Macromol. Sci., Chem.* **1975**, *9*, 1.
(35) Rao, S. P.; Ponratman, S.; Kapur, S. L.; Iyer, P. K. *J. Polym. Sci., Polym. Lett. Ed.* **1976**, *14*, 513.
(36) Mayo, F. R.; Walling, C. *Chem. Rev.* **1950**, *200*, 0.
(37) Chiellini, E.; Solaro, R.; Ledwith, A.; Galli, G. *Eur. Polym. J.* **1980**, *13*, 1654.
(38) Peat, I. R.; Reynolds, W. F. *Tetrahedron Lett.* **1972**, 1359.
(39) McCord, E. F.; Anton, W. L.; Wilczek, L.; Ittel, S. D.; Nelson, L. T. J.; Raffell, K. D. *Macromol. Symp.* **1994**, *86*, 47.
(40) Xie, S.; Natansohn, A.; Rochon, P. *Macromolecules* **1994**, *27*, 1885.
(41) DiMarzio, E. A.; Dowell, F. *J. Appl. Phys.* **1979**, *50*, 6061.
(42) Xie, S.; Natansohn, A.; Rochon, P. *Chem. Mater.* **1995**, *5*, 405.
(43) Altomare, A.; Ciardelli, F.; Ghiloni, M. S.; Solaro, R.; Tirelli, N. *Macromol. Chem. Phys.* **1997**, *198*, 1739.
(44) Carlini, C.; Garzoni, F. *Polymer* **1983**, *24*, 101.
(45) Chiellini, E.; Solaro, R.; Galli, G.; Ledwith, A. *Macromolecules* **1980**, *13*, 1118.
(46) Tinoco, I., Jr. *J. Am. Chem. Soc.* **1960**, *82*, 4785.
(47) Okamoto, K.; Itaya, A.; Kusabayashi, S. *Chem. Lett.* **1974**, 1167.
(48) Ciardelli, F.; Aglietto, M.; Carlini, C.; Chiellini, E.; Solaro, R. *Pure Appl. Chem.* **1982**, *54*, 521.
(49) Meng, X.; Natansohn, A.; Barrett, C.; Rochon, P. *Macromolecules* **1996**, *29*, 946.
(50) Shimomura, M.; Kunitake, T. *J. Am. Chem. Soc.* **1987**, *109*, 5175.
(51) Menzel, H.; Weichart, B.; Schmidt, A.; Paul, S.; Knoll, W.; Stumpe, J.; Fischer, T. *Langmuir* **1994**, *10*, 1926.
(52) Dhanabalan, A.; Balogh, D. T.; Riul, A., Jr.; Giacometti, J. A.; Oliveira, O. N., Jr. *Thin Solid Films* **1998**, *323*, 257.
(53) Bruno, T. J.; Svoronos, P. D. N. *CRC Handbook of Basic Tables for Chemical Analysis*; CRC Press: Boca Raton, FL, 1989; p 89.
(54) Angiolini, L.; Caretti, D.; Giorgini, L.; Salatelli, E. *e-Polym.* **2001**, no. 21.
(55) Green, M. M.; Park, J. W.; Sato, T.; Teramoto, A.; Lifson, S.; Selinger, R. L. B.; Selinger, J. V. *Angew. Chem., Int. Ed.* **1999**, *38*, 3138−3154.
(56) Bian, S.; Li, L.; Liu, W.; Viswanathan, N. K.; Samuelson, L.; Kumar, J.; Kim, D. Y.; Williams, J.; Tripathy, S. K. *J. Mater. Chem.* **1999**, *9*, 1941.

MA052232U